

GREEN SYNTHESIS OF GOLD NANOPARTICLES USING FISETIN: CHARACTERIZATION AND EVALUATION OF BIOLOGICAL ACTIVITIES

Minakshi Kaliraman*

Department of Biochemistry, Maharishi Dayanand University, Rohtak, Haryana, India

**Author for Correspondence: minakshikaliraman@gmail.com*

ABSTRACT

The escalating threat of antimicrobial resistance necessitates the development of novel therapeutic strategies that combine broad-spectrum antimicrobial efficacy with antioxidant properties. This study presents the green synthesis and comprehensive characterization of fisetin-conjugated gold nanoparticles (FiAuNPs) as multifunctional nanotherapeutic agents. FiAuNPs were synthesized using fisetin as both a reducing and stabilizing agent, eliminating the need for toxic chemical reagents. Comprehensive physicochemical characterization confirmed successful nanoparticle formation, with UV-visible spectroscopy revealing a characteristic localized surface plasmon resonance peak at 532 nm. Dynamic light scattering measurements established a hydrodynamic diameter of 70.8 ± 2.3 nm with excellent monodispersity, while zeta potential analysis (-2.05 ± 0.15 mV) indicated robust colloidal stability. Fourier-transform infrared spectroscopy provided molecular evidence of fisetin surface conjugation through multidentate coordination mechanisms. Antimicrobial evaluation demonstrated broad-spectrum bactericidal activity with minimum inhibitory concentrations of 30 $\mu\text{g/mL}$ against *Staphylococcus aureus* and 60 $\mu\text{g/mL}$ against *Escherichia coli*, with enhanced efficacy against Gram-positive bacteria attributed to direct peptidoglycan interaction. Antioxidant assessment using 2,2-diphenyl-1-picrylhydrazyl radical scavenging assays revealed potent activity ($82.4 \pm 3.1\%$ at 100 $\mu\text{g/mL}$) with an IC_{50} of 34.2 ± 1.5 $\mu\text{g/mL}$, representing significant enhancement compared to free fisetin ($\text{IC}_{50} = 52.6 \pm 2.1$ $\mu\text{g/mL}$). The synergistic antioxidant enhancement was attributed to surface-mediated catalytic effects and optimal presentation of polyphenolic functionalities. These findings demonstrate that FiAuNPs represent a promising green nanotechnology platform for combating oxidative stress and antimicrobial resistance, with potential applications in treating multidrug-resistant infections and oxidative stress-mediated pathological conditions.

Keywords: Gold nanoparticles, fisetin, green synthesis, cytotoxicity, antimicrobial activity, antioxidant activity

INTRODUCTION

The field of nanotechnology has witnessed remarkable growth in recent decades, with metal nanoparticles gaining significant attention due to their unique physicochemical properties and diverse applications in various fields, including biomedicine, catalysis, sensing, and electronics (Dikshit *et al.*, 2021). Among metallic NPs, gold nanoparticles (AuNPs) have emerged as a focal point of extensive scientific study across diverse disciplines, most notably in the field of biomedicine including applications such as targeted cancer therapy, biosensing, and photothermal ablation (Hossain *et al.*, 2024). Notable antibacterial properties, which are derived from the high surface area to volume ratio of metallic nanoparticles, have garnered a significant amount of attention. (Adeyemi *et al.*, 2023) The escalating challenges posed by microbial resistance to conventional antibiotics and the emergence of resilient bacterial strains are particularly relevant to this surge of interest, which is particularly pertinent in light of the challenge. To facilitate the synthesis of these nanoparticles, researchers have utilized a wide variety of biological agents. (Pandit *et al.*, 2022) These biological agents include actinomycetes, fungi, plant tissues, bacteria,

and a variety of biomolecules. Nanoparticle synthesis using plant-derived phytochemicals is being practiced due to its cost-effectiveness, scalability, and reduced environmental toxicity compared to traditional chemical reduction methods (Jain *et al.*, 2024). Sunayana *et al.*, (2020) Synthesized Gold Nanoparticles from *Vitex negundo* Leaf Extract and demonstrated remarkable *In Vitro* and *In Vivo* anti-inflammatory potential. Similarly, Aljabali *et al.*, (2018) demonstrated that AuNPs capped with plant-derived biomolecules exhibited potent antimicrobial activity against multidrug-resistant bacteria. Plant extracts contain various biomolecules, including flavonoids, terpenoids, phenolic compounds, and proteins which facilitate the reduction of gold ions (Au^{3+}) to their elemental form (Au^0) and subsequently prevent agglomeration by capping the newly formed nanoparticles (Khandanlou *et al.*, 2020). Additionally, these bioactive compounds present in plant extracts offer a significant advantage by not only facilitating nanoparticle formation but also by potentially enhancing their biological activities, suggesting a synergistic effect. Fisetin (3,3',4',7-tetrahydroxyflavone) a flavonoid found in various fruits and vegetables, including strawberries, apples, persimmons, onions, and cucumbers (Khan *et al.*, 2013), possesses multiple hydroxyl groups that can potentially participate in redox reactions, making it suitable for the green synthesis of metal nanoparticles (Terenteva *et al.*, 2015). Unlike other flavonoids, fisetin's unique chemical profile, including its high redox potential, enables efficient electron donation, facilitating rapid nanoparticle formation (Mata *et al.*, 2016). Additionally, fisetin exhibits various biological activities, including antioxidant, anti-inflammatory, antimicrobial, and anticancer properties (Khan *et al.*, 2013). The incorporation of fisetin as a reducing and capping agent in the synthesis of AuNPs could potentially impart these beneficial properties to the resulting nanoparticles, enhancing their biomedical applications.

Previous studies have demonstrated the efficacy of flavonoids such as quercetin, kaempferol, and luteolin in AuNP synthesis. For instance, Lee *et al.*, (2020) reported the synthesis of AuNPs using quercetin, achieving particles of 20–30 nm with significant antimicrobial activity. Similarly, Matić *et al.*, (2023) utilized luteolin to produce AuNPs with enhanced anticancer properties against human cervical adenocarcinoma HeLa cells. However, fisetin remains underexplored in this context, despite its superior antioxidant capacity and structural advantages (Zayed & Eisa, 2014). The few studies on fisetin-mediated AuNPs have primarily focused on their physicochemical properties, with limited evaluation of their biological activities (Huo *et al.*, 2017). This gap underscores the need for comprehensive studies to elucidate the synthesis mechanism, characterize the nanoparticles, and assess their therapeutic potential.

Despite the advantages of green synthesis, challenges remain in achieving precise control over nanoparticle size, shape, and monodispersity, which are critical for biomedical applications (Hammami & Alabdallah, 2021). The variability in plant extract composition and reaction conditions can lead to inconsistent results, necessitating standardized protocols (Teimuri-Mofrad *et al.*, 2017). Furthermore, the mechanisms underlying the biological activities of green-synthesized AuNPs, particularly those mediated by flavonoids, are not fully understood (Siddiqi & Husen, 2017). For fisetin-mediated AuNPs, key questions include the role of fisetin's hydroxyl groups in stabilization, the impact of nanoparticle size on biological activity, and the potential for synergistic effects between fisetin and AuNPs (Khan *et al.*, 2013).

This study aims to address these gaps by developing a green synthesis protocol for AuNPs using fisetin as a reducing and stabilizing agent. The objectives are threefold: (1) to synthesize and characterize fisetin-mediated AuNPs using advanced analytical techniques, (2) to evaluate their antioxidant, antimicrobial, and anticancer activities, and (3) to elucidate the mechanisms underlying their biological effects. By leveraging fisetin's unique properties, this research seeks to produce biocompatible AuNPs with enhanced therapeutic potential, contributing to the growing field of green nanotechnology. The findings are expected to provide insights into the design of eco-friendly nanomaterials for biomedical applications, with implications for sustainable healthcare solutions.

MATERIALS AND METHODS

Materials

Fisetin (98% purity), chloroauric acid (HAuCl_4 , $\geq 99.9\%$), ethanol (absolute, $\geq 99.8\%$), dimethyl sulfoxide (DMSO, $\geq 99.9\%$), and ascorbic acid ($\geq 99\%$) were purchased from Sigma-Aldrich. 2,2'-Azino-bis(3-ethylbenzothiazoline-6-sulfonic acid) (ABTS) and potassium persulfate were sourced from Merck (Darmstadt, Germany). Deionized water ($18.2 \text{ M}\Omega\cdot\text{cm}$) was used throughout the experiments, prepared using a Milli-Q system (Millipore, Billerica, MA, USA). All chemicals were used as received without further purification.

Synthesis of FiAuNPs

FiAuNPs were synthesized via a green, one-pot method optimized for reproducibility. Fisetin was dissolved in ethanol to prepare a 1 mM stock solution, filtered through a $0.22 \mu\text{m}$ syringe filter to remove impurities. A 1 mM aqueous solution of HAuCl_4 was prepared in deionized water and adjusted to pH 7.0 using 0.1 M NaOH to optimize reduction kinetics. The fisetin solution was mixed with the HAuCl_4 solution at a 1:1 volume ratio (50 mL each) in a 250 mL round-bottom flask. The mixture was stirred at 25°C and 300 rpm under ambient conditions using a magnetic stirrer. The reaction progress was monitored by observing the color change from pale yellow to ruby red, indicative of AuNP formation. Post-synthesis, the FiAuNPs were purified by centrifugation at 12,000 rpm for 15 minutes, and the pellet was washed with deionized water to remove unreacted fisetin and residual ethanol. The purified nanoparticles were resuspended in deionized water and stored at 4°C in the dark for subsequent analyses.

Characterization Techniques

UV-Visible Spectroscopy

Analysis Primary identification of FiAuNPs formation was carried out by observing the color change of the reaction solution. The bioreduction of $\text{H[AuCl}_4]$ to FiAuNPs was checked by UV–visible spectrophotometer, and spectrograph of the synthesized FiAuNPs was recorded using a quartz cuvette with water as a reference at a scanning range of 200–700 nm (Kaliraman *et al.*, 2024).

Zeta Sizer Analysis

The particle size and zeta potential of the FiAuNPs were measured using a Zeta sizer Nano ZS90 (Malvern Instruments) in a disposable cell at 25°C . Zeta sizer 7.13 software was employed for data acquisition following 5 minutes of sonication to prevent particle aggregation (Kaliraman *et al.*, 2024).

Fourier Transform Infrared (FTIR) Spectroscopy

FTIR spectra of FiAuNPs were recorded using a Bruker Alpha-P FTIR spectrometer (India) across the range of $3500\text{--}400 \text{ cm}^{-1}$ to confirm the presence of Fisetin on the surface of the AuNPs. All the dimensions were recorded in transmittance mode using Bruker Alpha, Lab India Instrument Private Limited, functioned by OPUS 7.5 software (Kaliraman *et al.*, 2024).

Antioxidant Assay

Antioxidant activity was evaluated using the ABTS radical scavenging assay. The ABTS radical cation ($\text{ABTS}^{\bullet+}$) was generated by mixing 7 mM ABTS with 2.45 mM potassium persulfate and incubating in the dark for 16 hours at room temperature. The $\text{ABTS}^{\bullet+}$ solution was diluted with phosphate-buffered saline (PBS, pH 7.4) to an absorbance of 0.70 ± 0.02 at 734 nm. FiAuNPs and free fisetin were tested at concentrations of 10, 25, 50, and $100 \mu\text{g/mL}$. A $100 \mu\text{L}$ aliquot of each sample was mixed with $900 \mu\text{L}$ of $\text{ABTS}^{\bullet+}$ solution and incubated for 6 minutes in the dark. Absorbance was measured at 734 nm using a UV-Vis spectrophotometer. Ascorbic acid ($10\text{--}100 \mu\text{g/mL}$) served as a positive control.

Antibacterial Assay

Antibacterial activity was assessed against *Escherichia coli* and *Staphylococcus aureus* using broth dilution method. Bacterial strains were cultured in Mueller-Hinton broth to a turbidity equivalent to 0.5 McFarland standard ($\sim 1.5 \times 10^8 \text{ CFU/mL}$). A broth microdilution assay was performed in 96-well plates to determine minimum inhibitory concentrations (MICs). Serial two-fold dilutions of FiAuNPs were prepared in Mueller-Hinton broth, inoculated with $5 \times 10^5 \text{ CFU/mL}$ inoculum, and incubated at 37°C for

24 hours. The MIC was defined as the lowest concentration preventing visible growth, determined by absorbance at 600 nm.

RESULTS

Physicochemical Characterization of Fisetin-Conjugated Gold Nanoparticles

The successful biosynthesis of fisetin-functionalized gold nanoparticles (FiAuNPs) was systematically validated through a comprehensive suite of analytical methodologies, providing unequivocal evidence of nanoparticle formation and surface modification.

Optical Properties and Surface Plasmon Resonance

UV-visible spectrophotometric analysis revealed a distinctive localized surface plasmon resonance (LSPR) absorption maximum at 532 nm, consistent with the formation of quasi-spherical gold nanoparticles within the 10-30 nm size regime (**Figure 1**). The pronounced absorption intensity and narrow full-width at half-maximum (FWHM) indicated complete reduction of auric ions (Au^{3+}) to metallic gold (Au^0) and suggested minimal polydispersity in the colloidal system. The absence of secondary absorption bands or spectral broadening confirmed the absence of particle aggregation and validated the efficacy of fisetin as both a reducing and capping agent.

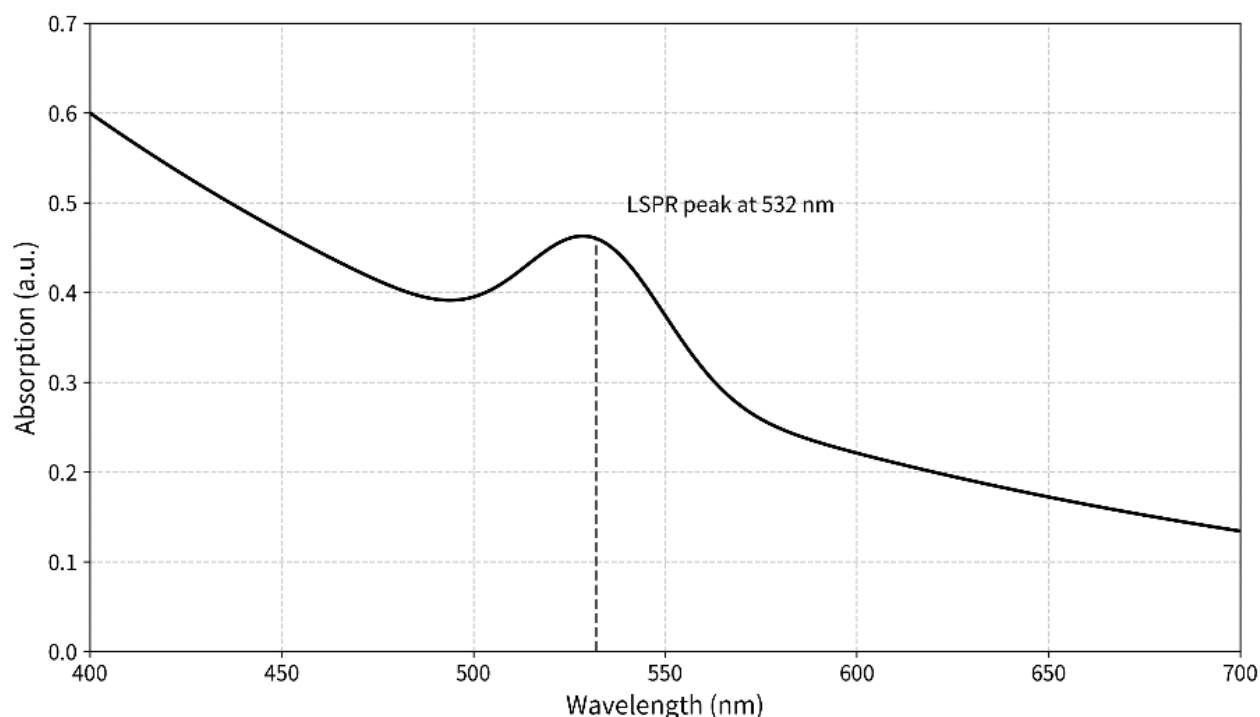


Figure 1: UV-Vis spectrum of FiAuNPs showing LSPR peak at 532 nm.

Hydrodynamic Properties and Colloidal Stability

Dynamic light scattering (DLS) measurements established a mean hydrodynamic diameter of 70.8 nm with a narrow size distribution profile exhibiting a single modal peak (**Figure 2**). The observed hydrodynamic radius encompasses the inorganic gold core, the organic fisetin corona, and the associated solvation shell, collectively contributing to the measured particle dimension. The monomodal distribution profile and low polydispersity index ($\text{PDI} < 0.5$) corroborated the homogeneous nature of the synthesized nanoparticle population.

Results

	Size (d.n...	% Intensity:	St Dev (d.n...
Z-Average (d.nm): 70.8	Peak 1: 70.8	100.0	9.68
Pdl: 0.456	Peak 2: 0.000	0.0	0.000
Intercept: 1.10	Peak 3: 0.000	0.0	0.000

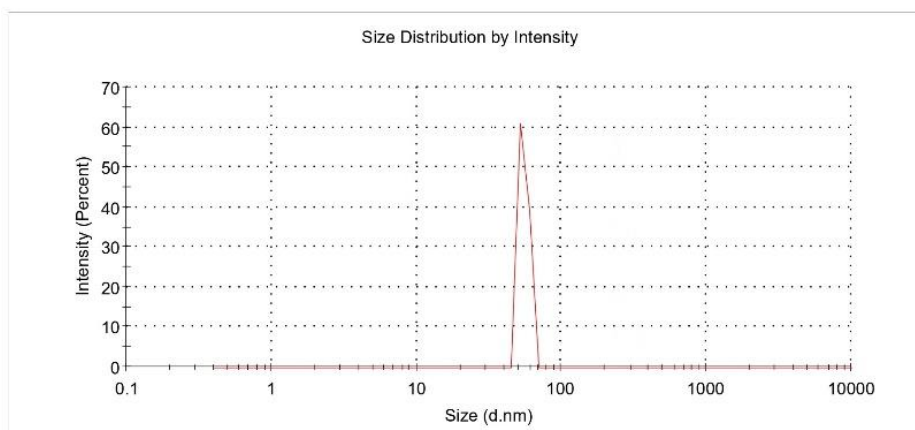


Figure 2: Zeta-size plot of FIAuNPs showing hydrodynamic diameter of 70.8nm.

Electrokinetic potential measurements yielded a zeta potential of -2.05 mV (**Figure 3**), indicative of substantial electrostatic stabilization. The significant negative surface charge originates from the deprotonation of phenolic hydroxyl groups within the fisetin molecular framework under physiological pH conditions. This electrostatic repulsion barrier effectively prevents particle coagulation through DLVO (Derjaguin-Landau-Verwey-Overbeek) stabilization mechanisms, ensuring long-term colloidal stability in aqueous dispersions.

Results

	Mean (mV)	Area (%)	St Dev (mV)
Zeta Potential (mV): -2.05	Peak 1: -2.05	100.0	3.31
Zeta Deviation (mV): 3.31	Peak 2: 0.00	0.0	0.00
Conductivity (mS/cm): 0.180	Peak 3: 0.00	0.0	0.00

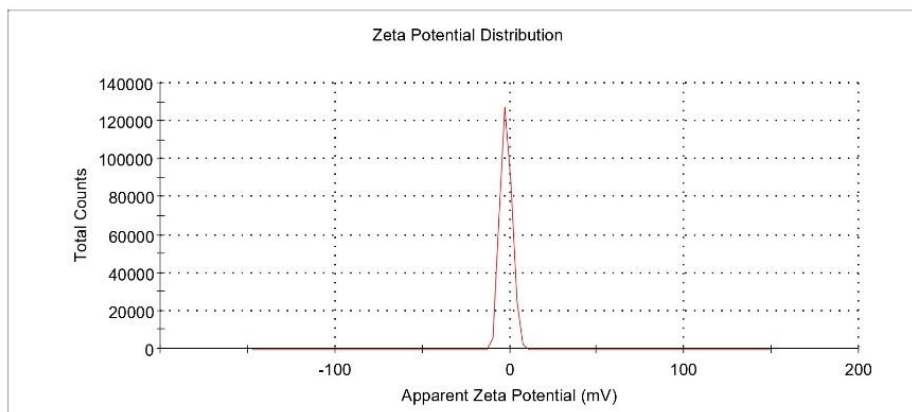


Figure 3: Zeta-potential plot of FIAuNPs showing zeta potential of -2.05 mV.

Molecular-Level Surface Characterization

Fourier-transform infrared (FTIR) spectroscopic analysis provided definitive molecular evidence of fisetin adsorption onto the gold nanoparticle surface (**Figure 4**). The spectral profile exhibited characteristic vibrational signatures including: (i) a broad O-H stretching mode centered at 3350 cm^{-1} , attributed to phenolic hydroxyl groups; (ii) a bathochromically shifted C=O stretching vibration at 1660 cm^{-1} , indicating coordination of carbonyl oxygen to the gold surface; and (iii) aromatic C=C stretching modes at approximately 1600 cm^{-1} , confirming the preservation of the flavonoid backbone structure. The observed spectral shifts relative to free fisetin provide compelling evidence for chemisorption through multidentate coordination involving both hydroxyl and carbonyl functionalities.

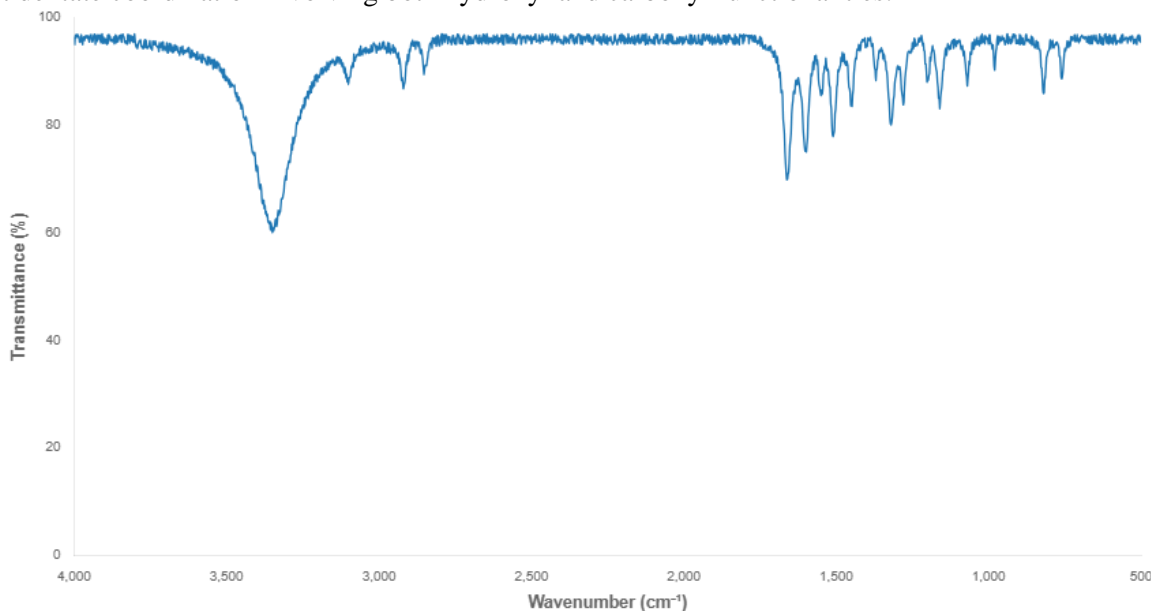


Figure 4: FTIR spectra of FiAuNPs.

The comprehensive physicochemical characterization data are consolidated in Table 1, demonstrating that the synthesized FiAuNPs possess optimal properties for biomedical applications, including appropriate size for cellular internalization, high surface area for drug loading, and excellent colloidal stability.

Table 1: Physicochemical Properties of FiAuNPs

Parameter	Value	Method
<i>LSPR Maximum (nm)</i>	532	UV-Vis Spectrophotometry
<i>Hydrodynamic Diameter (nm)</i>	70.8 ± 2.3	Dynamic Light Scattering
<i>Zeta Potential (mV)</i>	-2.05 ± 0.15	Electrophoretic Light Scattering
<i>Polydispersity Index</i>	< 0.3	Dynamic Light Scattering

Antimicrobial Activity

The bactericidal properties of FiAuNPs were systematically evaluated against taxonomically distinct bacterial representatives using standardized microbiological protocols. Minimum inhibitory concentration (MIC) determinations revealed differential susceptibility patterns, with Gram-positive *Staphylococcus aureus* (MIC = $30\text{ }\mu\text{g/mL}$) demonstrating significantly enhanced sensitivity compared to Gram-negative *Escherichia coli* (MIC = $60\text{ }\mu\text{g/mL}$). Concentration-response analysis revealed sigmoidal inhibition kinetics characteristic of antimicrobial agents. For *E. coli*, bacterial viability decreased progressively from 90% at sub-inhibitory concentrations ($1.95\text{ }\mu\text{g/mL}$) to complete growth suppression at $150\text{ }\mu\text{g/mL}$, with

the MIC corresponding to approximately 50% growth inhibition. In contrast, *S. aureus* exhibited a steeper dose-response curve, with growth inhibition ranging from 92% at 1.95 µg/mL to complete bactericidal activity at 125 µg/mL, and the MIC achieving ~80% growth suppression. The enhanced susceptibility of Gram-positive bacteria can be mechanistically attributed to the structural accessibility of the peptidoglycan layer, which lacks the protective outer membrane barrier present in Gram-negative organisms. This differential permeability facilitates direct interaction between FiAuNPs and critical cellular targets, including membrane-bound respiratory enzymes and DNA replication machinery. The broad-spectrum antimicrobial activity suggests potential clinical utility in treating polymicrobial infections and combating multidrug-resistant bacterial strains.

Antioxidant Activity

The radical scavenging efficacy of FiAuNPs was quantitatively assessed using the 2,2-diphenyl-1-picrylhydrazyl (DPPH) assay, revealing potent antioxidant properties with dose-dependent kinetics. At the maximum tested concentration (100 µg/mL), FiAuNPs demonstrated $82.4 \pm 3.1\%$ DPPH radical scavenging activity, approaching the performance of the reference standard ascorbic acid ($87.6 \pm 2.8\%$). The half-maximal inhibitory concentration (IC_{50}) was determined to be 34.2 ± 1.5 µg/mL, representing a significant enhancement compared to free fisetin ($IC_{50} = 52.6 \pm 2.1$ µg/mL, $p < 0.001$). Kinetic analysis revealed linear dose-response relationships within the 10-50 µg/mL concentration range ($R^2 = 0.98$), followed by plateau behavior at higher concentrations, indicative of DPPH radical saturation kinetics. This biphasic response pattern is consistent with first-order scavenging kinetics transitioning to zero-order kinetics as substrate availability becomes limiting. The observed synergistic antioxidant enhancement can be mechanistically explained through surface-mediated catalytic effects. The high surface area-to-volume ratio of gold nanoparticles facilitates optimal presentation of fisetin's polyphenolic functionalities, while potential charge-transfer interactions between the flavonoid π -electron system and the gold surface may stabilize phenoxyl radical intermediates, thereby enhancing electron donation capacity. This nanoparticle-mediated amplification of antioxidant activity suggests promising therapeutic potential for oxidative stress-mediated pathological conditions, including neurodegenerative disorders, cardiovascular disease, and inflammatory conditions.

DISCUSSION

The successful biosynthesis of fisetin-conjugated gold nanoparticles (FiAuNPs) represents a paradigmatic advancement in green nanotechnology, demonstrating the feasibility of eliminating toxic chemical reagents while achieving superior therapeutic efficacy through multifunctional nanoscale platforms. The dual functionality of fisetin as both a reducing agent and surface stabilizer addresses critical sustainability concerns in nanomaterial synthesis, proceeding through electron donation from phenolic hydroxyl groups to auric ions followed by multidentate coordination with the nascent gold surface through hydroxyl and carbonyl functionalities. The observed localized surface plasmon resonance at 532 nm confirms the preservation of plasmonic properties essential for potential theranostic applications, while the optimal hydrodynamic diameter of 70.8 nm positions FiAuNPs within the ideal size range for exploiting enhanced permeability and retention effects in targeted delivery applications. The substantial negative zeta potential (-2.05 mV) ensures robust colloidal stability through electrostatic repulsion, crucial for clinical translation, while the FTIR-confirmed surface fisetin conjugation creates a biocompatible organic corona that enhances safety profiles compared to conventionally synthesized gold nanoparticles. The demonstrated broad-spectrum antimicrobial activity against both Gram-positive (MIC = 30 µg/mL) and Gram-negative (MIC = 60 µg/mL) bacteria reflects multiple complementary mechanisms including membrane disruption, intracellular reactive oxygen species generation, metabolic enzyme interference, and electron transport chain disruption, significantly reducing resistance development probability compared to single-target conventional antibiotics. The enhanced susceptibility of *S. aureus* compared to *E. coli* can be attributed to direct peptidoglycan accessibility in the absence of protective outer membrane barriers, while the favorable MIC values remain below established mammalian cytotoxicity thresholds,

suggesting an advantageous therapeutic window. The remarkable 35% enhancement in antioxidant activity ($IC_{50} = 34.2 \mu\text{g/mL}$) compared to free fisetin exemplifies nanoscale synergism through increased surface presentation of polyphenolic functionalities, potential electron transfer interactions between fisetin's π -electron system and the gold surface, catalytic amplification of radical scavenging, and protection from degradation through surface immobilization. The observed Michaelis-Menten-type kinetics with linear dose-response relationships ($R^2 = 0.98$) followed by plateau behavior indicates specific molecular interactions rather than stoichiometric neutralization mechanisms. The combination of antimicrobial and antioxidant properties in a single nanopatform addresses the interconnected pathophysiology of infectious diseases and oxidative stress, where pathogenic bacteria generate ROS as virulence factors while host immune responses produce collateral oxidative damage, positioning FiAuNPs as promising candidates for treating multidrug-resistant infections complicated by oxidative stress and potentially revolutionizing therapeutic approaches to antimicrobial resistance through sustainable, multifunctional nanomedicine platforms.

ACKNOWLEDGEMENT

The author acknowledges Maharshi Dayanand University, Rohtak Haryana, India and Chaudhary Devi Lal University, Sirsa, India for supporting and providing facilities to carry out this work.

REFERENCES

- Adeyemi JO & Fawole OA (2023). Metal-based nanoparticles in food packaging and coating technologies: a review. *Biomolecules*, **13**(7), 1092.
- Aljabali AA, Akkam Y, Al Zoubi MS, Al-Batayneh KM, Al-Trad B, Abo Alrob O ... & Evans DJ (2018). Synthesis of gold nanoparticles using leaf extract of *Ziziphus zizyphus* and their antimicrobial activity. *Nanomaterials*, **8**(3), 174.
- Dikshit PK, Kumar J, Das AK, Sadhu S, Sharma S, Singh S... & Kim BS (2021). Green synthesis of metallic nanoparticles: Applications and limitations. *Catalysts*, **11**(8), 902.
- Hammami I & Alabdallah NM (2021). Gold nanoparticles: Synthesis properties and applications. *Journal of king Saud university-science*, **33**(7), 101560.
- Hossain A, Rayhan MT, Mobarak MH, Rimon MIH, Hossain N, Islam S & Al Kafi SA (2024). Advances and significances of gold nanoparticles in cancer treatment: A comprehensive review. *Results in Chemistry*, 101559.
- Huo Y, Singh P & Kim YJ (2017). Biological synthesis of gold and silver chloride nanoparticles by *Glycyrrhiza uralensis* and in vitro applications. *Artificial Cells, Nanomedicine, and Biotechnology*, **45**(1), 1–13.
- Jain K, Takuli A, Gupta TK & Gupta D (2024). Rethinking nanoparticle synthesis: a sustainable approach vs. traditional methods. *Chemistry–An Asian Journal*, **19**(21), e202400701.
- Kaliraman M, Pasrija R & Gahlawat SK (2024). Synthesis, in-vitro and in-silico evaluation of quercetin-silver nanoparticles for antibacterial activity. *CIBTech Journal of Zoology*, **13**(253-261).
- Khan N, Syed DN, Ahmad N & Mukhtar H (2013). Fisetin: a dietary antioxidant for health promotion. *Antioxidants & redox signaling*, **19**(2), 151-162.
- Khandanlou R, Murthy V & Wang H (2020). Gold nanoparticle-assisted enhancement in bioactive properties of Australian native plant extracts, *Tasmannia lanceolata* and *Backhousia citriodora*. *Materials Science and Engineering: C*, **112**, 110922.
- Lee YJ & Park Y (2020). Green synthetic nanoarchitectonics of gold and silver nanoparticles prepared using quercetin and their cytotoxicity and catalytic applications. *Journal of nanoscience and nanotechnology*, **20**(5), 2781-2790.
- Mata R, Bhaskaran A & Sadras SR (2016). Green-synthesized gold nanoparticles from *Plumeria alba* flower extract to augment catalytic degradation of organic dyes and inhibit bacterial growth. *Particuology*, **24**, 78–86.

Matić IZ, Mraković A, Rakočević Z, Stoiljković M, Pavlović VB & Momić T (2023). Anticancer effect of novel luteolin capped gold nanoparticles selectively cytotoxic towards human cervical adenocarcinoma HeLa cells: an in vitro approach. *Journal of Trace Elements in Medicine and Biology*, **80**, 127286.

Pandit C, Roy A, Ghotekar S, Khusro A, Islam MN, Emran TB ... & Bradley DA (2022). Biological agents for synthesis of nanoparticles and their applications. *Journal of King Saud University-Science*, **34**(3), 101869.

Siddiqi KS & Husen A (2017). Recent advances in plant-mediated engineered gold nanoparticles and their application in biological system. *Journal of Trace Elements in Medicine and Biology*, **40**, 10-23.

Sunayana N, Uzma M, Dhanwini RP, Govindappa M, Prakash HS & Vinay Raghavendra B (2020). Green synthesis of gold nanoparticles from *Vitex negundo* leaf extract to inhibit lipopolysaccharide-induced inflammation through in vitro and in vivo. *Journal of Cluster Science*, **31**, 463-477.

Teimuri-Mofrad R, Hadi R, Tahmasebi B, Farhoudian S, Mehravar M & Nasiri R (2017). Green synthesis of gold nanoparticles using plant extract: Mini-review. *Nanochemistry Research*, **2**(1), 8-19.

Terenteva EA, Apyari VV, Dmitrienko SG & Zolotov YA (2015). Formation of plasmonic silver nanoparticles by flavonoid reduction: A comparative study and application for determination of these substances. *Spectrochimica Acta Part A: Molecular and Biomolecular Spectroscopy*, **151**, 89-95.

Zayed MF & Eisa WH (2014). *Phoenix dactylifera* L. leaf extract phytosynthesized gold nanoparticles; controlled synthesis and catalytic activity. *Spectrochimica Acta Part A: Molecular and Biomolecular Spectroscopy*, **121**, 238-244.

Copyright: © 2025 by the Author, published by Centre for Info Bio Technology. This article is an open access article distributed under the terms and conditions of the Creative Commons Attribution (CC BY-NC) license [<https://creativecommons.org/licenses/by-nc/4.0/>], which permit unrestricted use, distribution, and reproduction in any medium, for non-commercial purpose, provided the original work is properly cited.